Hard Photodisintegration of a Proton Pair

The Jefferson Lab Hall A Collaboration

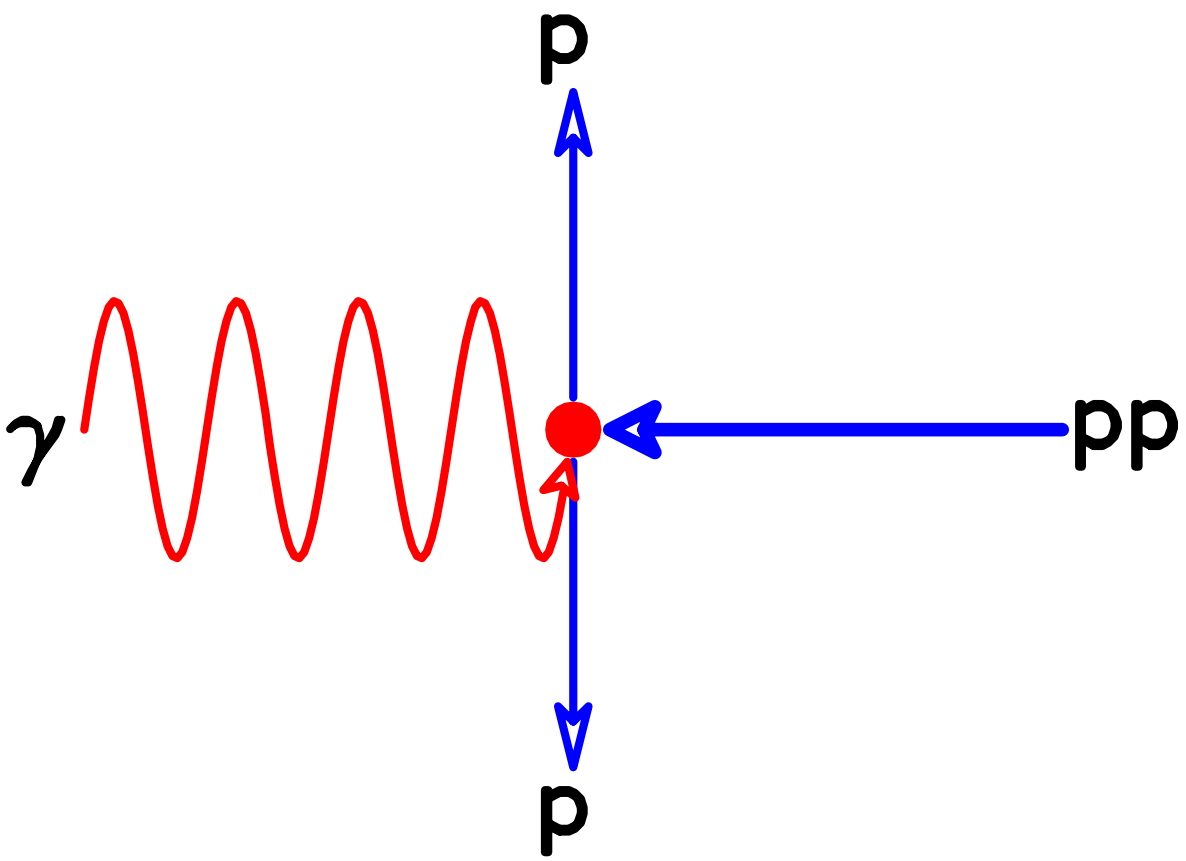

Jefferson Lab PAC 23, January 2003

D. Margaziotis
California State University, Los Angeles, CA USA

D. Dutta, H. Gao, W. Xu
Duke University, Durham, NC 27708 USA

P. Markowitz, M. Sargsian
Florida International University, Miami, FL 33199 USA

R. de Leo, L. La Gamba
INFN Bari, ITALY

F. Cusanno, S. Frullani, F. Garibaldi, M. Iodice, G.M. Urcioli
INFN Roma, ITALY

J.P. Chen, D.W. Higinbotham, S. Nanda, B. Reitz, B. Wojtsekhowski, S. Wood
Jefferson Lab, Newport News, VA 23606 USA

J.W. Watson
Kent State University, Kent, OH USA

S. Širca
University of Ljubljana, Jadranska 19, 1000 Ljubljana, SLOVENIA

W. Bertozzi, O. Gayou, S. Gilad, L. Zhu
Massachussetts Institute of Technology, Cambridge, MA 02139 USA

V. Punjabi
Norfolk State University, Norfolk, VA USA

L. Weinstein
Old Dominion University, Norfolk, VA 23529 USA

L. Bimbot
IPN Orsay B.P. n1 F-91406 Orsay FRANCE

M. Strikman
Pennsylvania State University, University Park, PA 16802 USA

E. Brash
University of Regina, Regina, CA

F. Benmokhtar, C. Glashausser, R. Gilman (contact person),
X. Jiang, G. Kumbartzki, K. McCormick, R. Ransome, J. Yuan
Rutgers University, Piscataway, NJ 08854-8019 USA

A.J. Sarty
St. Mary's University, Halifax, Nova Scotia B3H 3C3 CANADA

L. Frankfurt, E. Piasetzky (spokesperson)
Tel Aviv University, Tel Aviv, Israel

F. Butaru, S. Choi, Z.-E. Meziani, K. Slifer, P. Solvignon, H. Yao
Temple University, Philadelphia, PA USA

ABSTRACT

Jefferson Lab has devoted significant time in several highly-rated experiments to investigate high-energy, hard photodisintegration of the deuteron. The experiments test our ability to understand the transition region at intermediate energies, in which it is generally expected that it will be difficult to formulate meson-baryon theories, but in which quark-gluon theories might be relevant. At present, it does appear that hard deuteron photodisintegration is an intractable problem in meson-baryon theories, and that the quarks are the relevant degrees of freedom, but they cannot be described through perturbative QCD (pQCD). Several nonperturbative quark models have been formulated, and are in need of further testing. In this proposal, we request time to investigate a related process, the hard photodisintegration of a pp pair, in the ^{3}He nucleus. Measuring the photodisintegration of a pp pair provides important complementary information that will test the validity of the nonperturbative quark models.

We propose to measure both the energy dependence at $\theta_{\rm c.m.} = 90^\circ$ and the angular distribution near 90° c.m. for the hard photodisintegration of a pp pair in ^{3}He. The proposed measurement utilizes the special features of the photoabsorption process, the ^{3}He structure, and the pp interaction at high energy **to study the dynamics of the process, and to examine the validity of the impulse approximation** to see if it is the correct description of the hard process. In particular, **if the photodisintegration amplitude can be factorized so that it is related to the NN scattering amplitude, then the oscillations seen in pp scattering will also appear in the $\gamma\ ^3\mathrm{He} \to pp + n$ reaction**. In contrast, the oscillations are smaller and less certain in the pn channel, and cannot be clearly seen in deuteron photodisintegration. This proposal builds upon the knowledge learned from deuteron photodisintegration to see if a general understanding of hard exclusive nuclear photoreactions is possible.

The experiment is proposed for, and can only run in, Hall A. Required beam energies are $2-5$ GeV. The total time request is 320 hours, just over 13 days. The experiment uses existing equipment, such as the photon radiator, the Hall A ^{3}He gas target, and the two HRS spectrometers, to detect the two outgoing high-energy protons in coincidence. Based on our previous experience in Hall A with photoreactions such as $\gamma d \to pn$, $\gamma p \to p\pi^0$, $\gamma p \to \pi^+ n$, and $\gamma n \to p\pi^-$, which includes both singles and coincidence measurements, we see no significant issues of experimental feasibility. The experiment requires no new equipment or development time, and could run at almost any time the cryotarget is installed in Hall A.

In the following sections we review the scientific motivation and experimental details of the proposal. We discuss the deuteron photodisintegration data and scaling, the NN data, why we wish to measure ^{3}He photodisintegration, the ^{3}He photodisintegration prediction, nuclear corrections, and the neutron α distribution. In the experimental sections, we discuss the choice of beam energies, the choice of Hall A, equipment details, rates and backgrounds, systematic uncertainties, and the beam time request.

1 Scientific background and motivation

1.1 Overview

We define a hard photodisintegration of a nucleon pair as a process in which a high energy photon is absorbed by a nucleon pair and as a result the pair is disintegrated by emitting two nucleons with large transverse momenta, greater than about 1 GeV/c. As defined, in this process the Mandelstam parameters s, the square of the total energy in the c.m. frame, and t, the four-momentum transfer from the photon to the nucleon, are large. We propose here to study the energy dependence of the photodisintegration of a proton pair in ^{3}He. We also propose to measure the angular distribution near 90° in the $\gamma - pp$ c.m. system. The focus of the proposed measurements is to study the hard breakup dynamics.

In an impulse approximation picture with hadronic degrees of freedom, the high energy photon is absorbed by one of the nucleons. Momentum conservation causes the nucleon that absorbs the photon to recoil with a large momentum in the photon direction. In the end, the two nucleons emerge, both with very large momentum in the transverse direction. The question is: how is this very large transverse momentum acquired? In principle, within this impulse approximation description, there are two basic ways, illustrated in Fig. 1, that it can happen:

- *Breaking a transverse compact object formed before the absorption*
  The disintegrated pair was compact in the transverse direction and the very large relative transverse momentum between the nucleons is what leads to the two nucleons recoiling with such large momenta. This must be a very minute part of the pair wave function since the transverse momenta are about 20 times larger than the average momentum of a nucleon in a deuteron.

- *Hard Rescattering*
  The nucleon that absorbs the photon acquires a large longitudinal momentum. It then interacts with the other member of the pair. This also is a rare case (large c.m. scattering angle) in which the pair recoils in the transverse direction. It is a hard rescattering process (FSI).

Photodisintegration of a pn pair, the deuteron, has now been extensively studied. Data are available for high-energy cross sections at photon energies up to 5 GeV [1, 2, 3, 4], including, for energies up to 2.5 GeV, "complete" angular distributions [5, 6] and recoil polarizations [7]. Here we propose to investigate the photodisintegration of a pp pair in ^{3}He. **The proposed measurement utilizes the special features of the photoabsorption process, the ^{3}He structure, and the pp interaction at high energy to verify that the impulse approximation is the correct description of the hard process, and also to determine if one of the options mentioned above is the dominant process.**

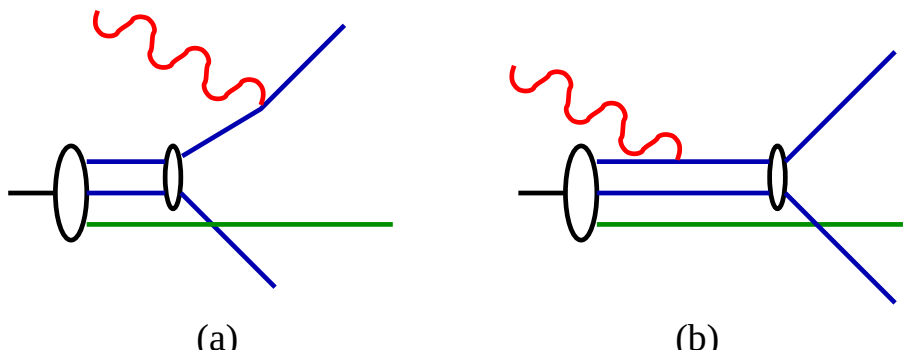

Figure 1: *Possible reaction mechanisms, with hadronic degrees of freedom.* (a) - *The left panel illustrates hard photodisintegration of* ^{3}*He through initial state correlations. High-momentum components of the wave function, related to a spatially compact configuration, lead to the protons having large transverse momenta even before the photon is absorbed.* (b) - *The right panel illustrates hard photodisintegration arising through a final state interaction between the two protons. The two protons acquire large transverse momenta when scattering from each other, after the photon is absorbed. In each case, the neutron is shown as a spectator.*

1.2 Hard photodisintegration of the deuteron and scaling of cross sections

High energy photodisintegration of the deuteron at 90° c.m. provides an efficient way to reach the hard regime (Mandelstam $-t$ and $-u \geq 2$ GeV^2) in a nuclear reaction – see e.g. [8]. In this reaction, Mandelstam s is given by

$$s_{\gamma D} = (P_\gamma + P_D)^2 = M_D^2 + 2M_D E_\gamma, \tag{1}$$

where P_γ and P_D are the photon and deuteron momentum four vectors, respectively, M_D is the deuteron mass, and E_γ is the photon energy in the laboratory frame. For 90° c.m. scattering, $t = u = -\frac{s-M_D^2}{2} + M_N^2$. As is shown in Table 1, these kinematics allow access to a large range of s and t at photon beam energies already available at Jefferson Lab.

To emphasize the ability of this reaction to reach large s, we observe that to reach the same s in pn scattering, one needs an incident nucleon lab momentum about a factor of two larger than that of the photon in the $\gamma d \to pn$ reaction.

One of the main motivations for studies of high-energy wide-angle exclusive reactions was the prediction [9] that the differential cross section scales as

$$\frac{d\sigma}{dt}_{AB\to CD} \sim s^{-(n_A+n_B+n_C+n_D-2)} f\left(\frac{t}{s}\right) \tag{2}$$

where n_A, n_B, n_C, and n_D are the number of constituents inside the particles A, B, C, and D, respectively. Eq. 2, which is known as the *dimensional counting rule*, was first derived in 1973 [9] in asymptotic form ($s \to \infty$, $\frac{t}{s}$ fixed), using dimensional analysis.

Table 1: *Kinematics for hard photodisintegration of an NN pair at $\theta_{\rm c.m.} = 90°$, in the γNN system, and the equivalent incident nucleon momentum for NN scattering. t and p_T are relativistic invariants that characterize the momentum transferred from the photon to each nucleon; t is the four-momentum transferred from the photon to the proton, and p_T is the transverse momentum transferred.* $\mathrm{P_{beam}}$ *is the nucleon lab momentum in NN scattering that provides the same s.*

E_γ	s	t	p_T	$\mathrm{P_{beam}}$
[GeV]	[GeV^2]	[GeV^2]	[GeV/c]	[GeV/c]
2	11.0	-2.9	1.4	4.8
2.5	13.0	-3.8	1.5	5.9
3	14.8	-4.75	1.7	6.9
4	18.5	-6.6	1.9	8.9
5	22.3	-8.5	2.2	10.9
2.06	11.3	-3.0	1.4	5
4.5	20.6	-7.5	2.0	10
7.0	30.0	-12.2	2.6	15
9.5	39.3	-16.9	3.0	20

This description was followed by a more rigorous pQCD derivation [10], which assumed that the constituents are the valence quarks interacting through the hard gluon exchange. Analyses of hard hadronic reactions demonstrated that the number of constituents indeed coincided with the number of valence quarks in the hadrons (quark counting). There was great excitement initially that these reactions probe the onset of pQCD at the intermediate range of transferred momenta, $-t$ and $-u \geq 2-3$ GeV^2. However the attempts to describe the absolute values of cross sections within pQCD were unsuccessful, as they strongly underestimated the magnitudes of the cross sections. On the other hand, calculations based on models of nonperturbative QCD [11, 12] demonstrated that the observed scaling may not indicate the onset of the pQCD regime, and probably nonperturbative QCD is still strongly dominating.

Based on the phenomenological success of the quark counting rule, Brodsky and Chertok [13] suggested that the onset of the quark degrees of freedom in hard exclusive nuclear reactions will be manifested through the same scaling rule of Eq. 2. Indeed, the scaling observed for high-energy deuteron elastic and photodisintegration reactions is in agreement with the quark counting rule. In particular, for high-energy deuteron photodisintegration, Eq. 2 predicted an energy dependence of s^{-11} which is in agreement with the data [1, 2, 3, 4] starting at $E_\gamma \geq 1$ GeV for $\theta_{\rm c.m.} = 90°$, and starting at other angles once $p_T \geq 1.3$ GeV. However, as was the case for hard exclusive hadronic reactions, for nuclear reactions pQCD also strongly underestimates the cross section – an example

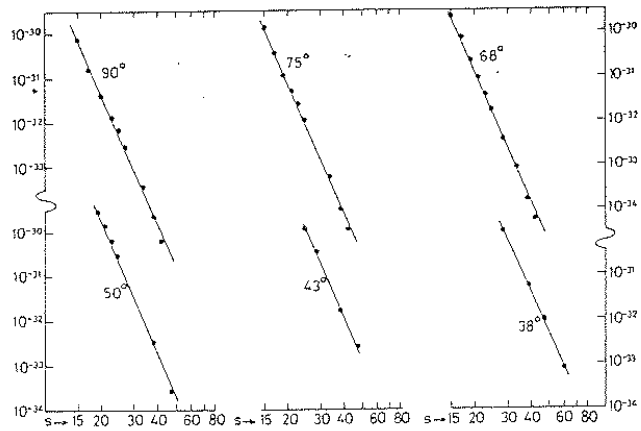

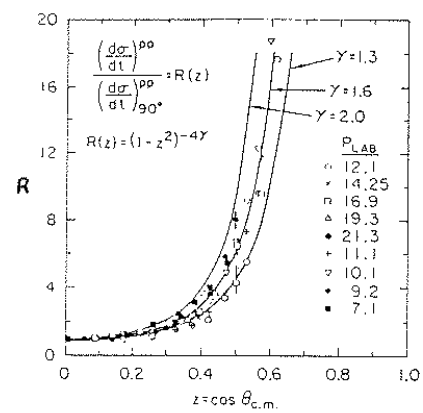

Figure 2: *Data for pp elastic scattering along with fits based on theoretical predictions.* Left - *Figure from Ref. [19] showing the s-dependence of* $\frac{d\sigma}{dt}(pp)$ *at various* $\theta_{\rm c.m.}$ *values. The fits are based on Eq. 2 with* $n_A + n_b + n_c + n_D - 2 = 9.7$. Right - *Figure from Ref. [18] showing the angular dependence of* $\frac{d\sigma}{dt}(pp)$*, normalized to its value at* $\theta_{\rm c.m.} = 90°$*, at various incident momentum values. The fits are based on Eq. 3.*

is the deuteron elastic form factor [14].

Thus, it is fair to state that although the observation of the scaling of Eq. 2 indicates the onset of the quark-gluon degrees of freedom in a reaction, the appropriate underlying physics is nonperturbative QCD, rather than pQCD. A variety of theoretical models exist which attempt to incorporate the nonperturbatice QCD effects. The best descriptions for the high-energy deuteron photodisintegration data are the QCD rescattering model of Sargsian and collaborators [15] and the quark-gluon string (QGS) model of Kondratyuk and collaborators [16]. To date, there are no successful meson-baryon calculations for the high energy data. For a recent review, see [17].

1.3 The *pp* scattering data, scaling, and deviations from scaling

For high-energy, large-angle $pp \to pp$ elastic scattering, according to the quark counting rule of Eq. 2, one expects $\frac{d\sigma}{dt} \sim s^{-10}$. Note that a constant value of t/s in Eq. 2 is equivalent to a constant c.m. scattering angle. The data are globally consistent over a large number of decades with the power law, as can be seen in Fig. 2.

No rigorous pQCD calculation has been performed as yet for the function $f\left(\frac{t}{s}\right)$ in Eq. 2. However, there is a calculation within the pQCD-based, constituent-interchange model (CIM) [18] which predicts

$$f\left(\frac{t}{s}\right) \equiv f(\cos\theta_{\rm c.m.}) \sim (1 - \cos^2\theta_{\rm c.m.})^{-4\gamma} \tag{3}$$

where γ can be in the range 1.3 - 2.0 . In Fig. 2 we show $pp \to pp$ data [19] in the kinematic region of interest, along with fits which are based on Eqs. 2 and 3.

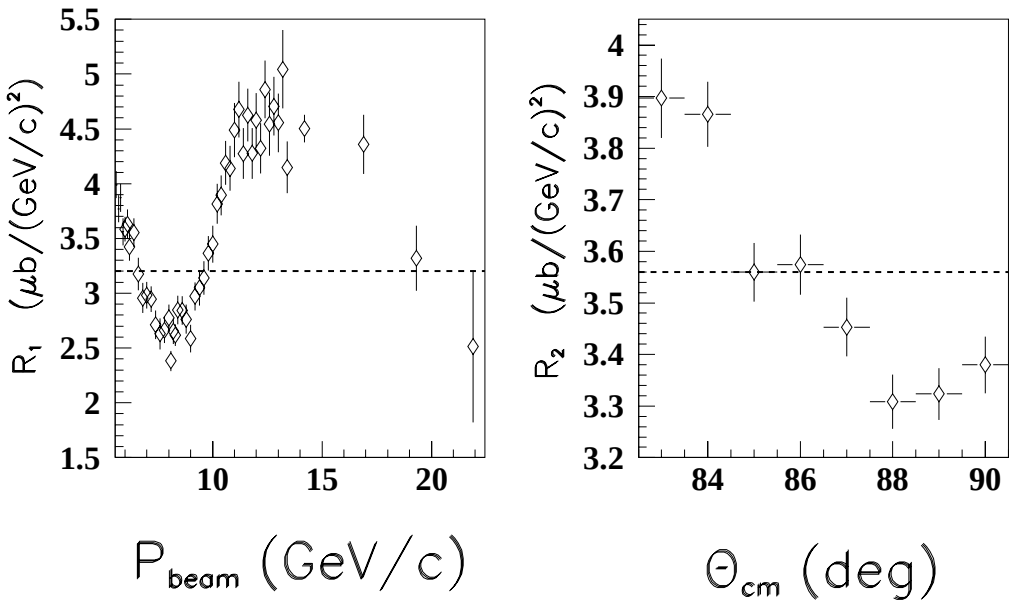

Figure 3: *Scaled $pp \to pp$ differential cross sections. The dashed lines represent perfect scaling. Their vertical position is arbitrary.* Left - $R_1 = \left(\frac{s}{s_0}\right)^{10} \frac{d\sigma}{dt}(pp)$, *with s_0 = 13 GeV^2 at $\theta_{\rm c.m.}$ = 90°, versus the proton laboratory-frame incoming momentum. The relation between the incident momentum in pp scattering and the γpp kinematics is given in Table 1.* Right - $R_2 = (1 - \cos^2\theta_{\rm c.m.})^{4\gamma} \frac{d\sigma}{dt}(pp)$, *with γ = 1.6 at p_{lab} = 5.9 GeV/c, versus $\theta_{\rm c.m.}$.*

Figure 2 shows that the data are globally consistent with Eqs. 2 and 3. However, it was already noted in 1974 [20] that a more detailed examination of the data indicated significant deviations from Eq. 2. This is seen clearly in Fig. 3, where we plot the "scaled" pp elastic scattering differential cross section versus incident momentum and $\theta_{\rm c.m.}$. By "scaled" we mean that we multiply the cross sections by their global kinematic dependencies predicted by Eqs. 2 and 3.

The deviation of the $\frac{d\sigma}{dt}(\theta_{\rm c.m.})$ from Eq. 3 has not been discussed previously, whereas the deviation of pp elastic data at $\theta_{\rm c.m.} = 90°$ from the simple scaling law of Eq. 2 has prompted numerous theoretical interpretations. The first attempts to explain the data [20, 21] were in terms of hadronic degrees of freedom, within diffractive scattering models. We discuss below two theoretical interpretations inspired by QCD. Their common element is that at the currently accessible energies, there are significant additional components which interfere with the pQCD amplitude.

Ralston and Pire [22] suggested that the pp elastic cross section is a combination of two components. One component follows the dimensional counting rule of Eq. 2, and is associated with small size fluctuations of hadrons. The second component is the multiple-scattering component discussed by Landshoff [23], which describes hadronic scattering as the independent scattering of **all** valence quarks. The main feature of the latter mechanism is that the hadrons retain their normal size during the interaction. The interference between these two components is governed by the so-called chromo-Coulomb phase, and results in oscillations around the scaled pp cross section – see Fig. 3.

Brodsky and deTeramond [24] suggested that the oscillations in the pp cross section are due to the presence of two broad resonances (or threshold enhancements) at $m^* = 2.55$ GeV and $m^* = 5.08$ GeV. The sum of the resonance amplitudes and the standard pQCD amplitudes gives rise to the deviation from scaling in the range $\mathrm{P_{beam}} = 5.5$ - 13.4 GeV/c. As in the previous model, the resonances are associated with standard size hadrons as opposed to small size fluctuations in the pQCD amplitudes. For a review of wide-angle processes, see [18].

1.4 Why the $\gamma\, {}^3\mathrm{He} \to pp + n$ reaction?

In this proposal, we focus on the possibility that the hard photodisintegration of an NN pair can be related theoretically to the NN hard scattering amplitudes. If the photodisintegration process at $E_\gamma > 2 - 2.5$ GeV can be described as a factorization of the amplitude into parts involving the conventional nucleon pair wave function times the cross section for NN scattering – see Eq. 5 below – any unique signature of the NN interaction should show itself directly in the hard photodisintegration. This is the underlying physics of the QCD hard rescattering model (HRM) [15]. In contrast, there is no such direct relation between the NN amplitudes and the photodisintegration process in the QGS model.

Figure 4 demonstrates the comparison of the calculations based on the HRM with the available data for deuteron disintegration at $\theta_{\mathrm{c.m.}} = 90°$. No adjustable parameter is used in these calculations. For the pn scattering cross section, a fit to the existing pn data has been used. The general agreement between the data and the absolute cross section calculated in the HRM is clear. Because of the relatively poor accuracy of hard-scattering pn data, the overall accuracy of the calculation is on the level of 20% – this is why the calculation is shown as an error band in the figure. As a result, it is very challenging to test the model based on the unique feature of hard pn scattering. Besides, hard scattering pn data exist only at lab momenta up to 12 GeV/c, which corresponds to $E_\gamma \approx 6$ GeV. Therefore the extension of the $\gamma d \to pn$ reaction to higher energies will not allow further testing of the model.

Also shown in Fig. 4 is the QGS model of Kondratyuk and collaborators [16]. The calculation shown underpredicts the data at high energies, but it is sensitive to the Regge trajectory used. While better calculations are possible for these data, the particular calculation shown is consistent with those that best fit the forward-angle data. The

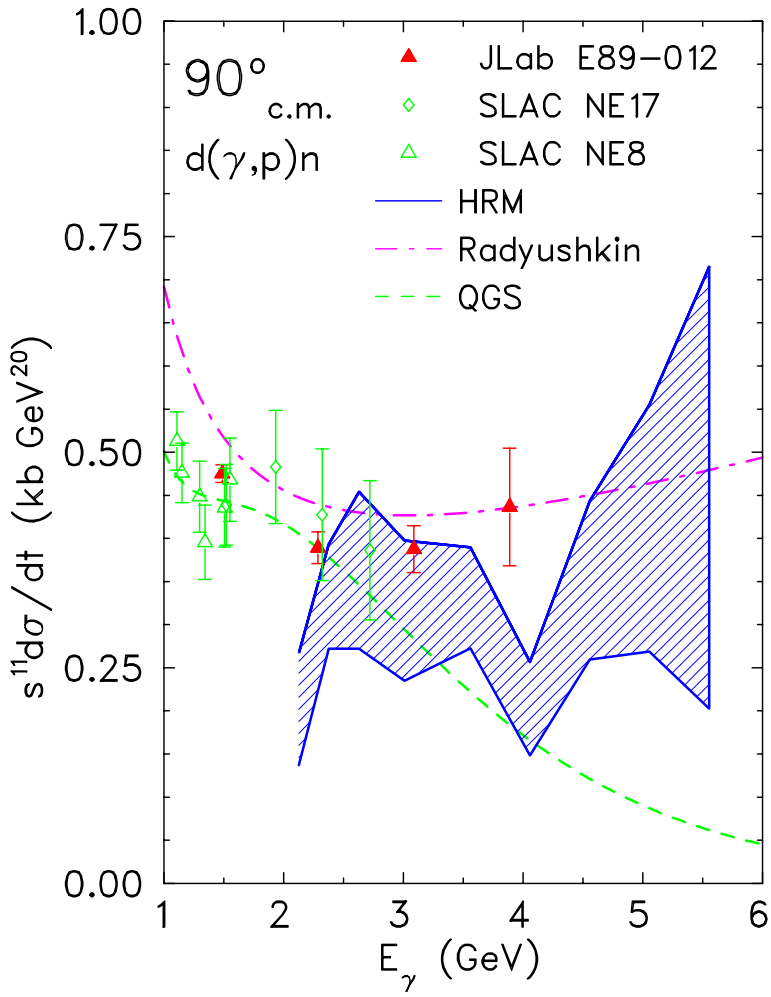

Figure 4: *The energy dependence of* $s^{11}\frac{d\sigma}{dt}$ *for 90° c.m. photodisintegration of the deuteron. See text for details.*

calculation shown uses a nonlinear trajectory, as opposed to the more familiar linear trajectories, which have the more straightforward interpretation as a sum over the exchange of a family of particles. While an oscillating trajectory could produce some oscillations in the cross section, no suggestion of or justification for such a trajectory has ever been made, to our knowledge.

The Radyushkin model [25] is based on the idea that the photon interacts with a pair of quarks being interchanged between the two nucleons. An analysis of this hard interaction then shows that the reaction has leading kinematic dependences proportional to a transition $p \leftrightarrow n$ form factor – presumably similar to the dipole form factor – to the fourth power times phase space factors. There is no absolute normalization predicted by the model; instead it is normalized to the data point at 4 GeV and 90°. With this normalization, the formula manages to largely reproduce the energy and angle dependences

of hard deuteron photodisintegration, for $E_\gamma > 1.5$ GeV.

The crucial difference between the hard rescattering model and the QGS or quark interchange models is that the former predicts oscillations in the energy dependence that arise from the pn interaction, whereas the latter models both predict smooth energy and angle dependences. **Unfortunately, the precision of the pn and the $\gamma d \to pn$ data are insufficient to show if oscillations are indeed present**, and thus one is unable to choose between these approaches purely from the experimental data.

The importance of the pp system compared to the deuteron (pn pair) is that the hard pp elastic scattering data are much better measured than are the pn data, and have more prominent oscillations. The oscillations are the unique features of the pp interaction that we will use as signatures to determine whether the impulse approximation to hard scattering is correct and to test the nonperturbative quark models proposed to explain deuteron photodisintegration. The observation of oscillations, directly correlated to those in pp elastic scattering, would be a clear confirmation of the factorization of the amplitude used in the HRM.

Figure 5 demonstrates the much better quality of the pp elastic scattering data as compared to the pn data.[1] The uncertainties in the pp data are much smaller. The pn data have much larger uncertainties, and if any oscillations exist, they are not cleanly observed. Thus, as a test of factorization, it is evident that one would prefer photodisintegration of a pp pair, rather than a pn pair.

In the present proposal we attempt to extend the data that tests these ideas from the pn system of the deuteron to the pp system. The ^{3}He nucleus is the simplest available system that allows one to study the photodisintegration of a proton pair. Thus, we propose to measure the reaction

$$\gamma +^3 \mathrm{He} \to pp + n \tag{4}$$

in which we define the measurement conditions so that the neutron in ^{3}He can be considered, at least approximately, as a static spectator, while two protons are produced at 90° in the c.m. frame of the γpp system. This is done in the analysis by reconstructing the missing neutron momentum, and selecting events in which the neutron has a small momentum, less than 100 MeV/c, consistent with the neutron having been a spectator.

[1] In the HRM, the photodisintegration data are related to NN data at the same s_{NN} and t_N – see Eq. 5. The data shown are for 60° scattering in the NN c.m. system, which approximately matches the momentum transfer of 90° scattering in the γNN c.m. system. Thus, the data of Fig. 5 are the data that enter Eq. 5 below to describe the $\theta_{\mathrm{c.m.}} = 90°$ γpp scattering.

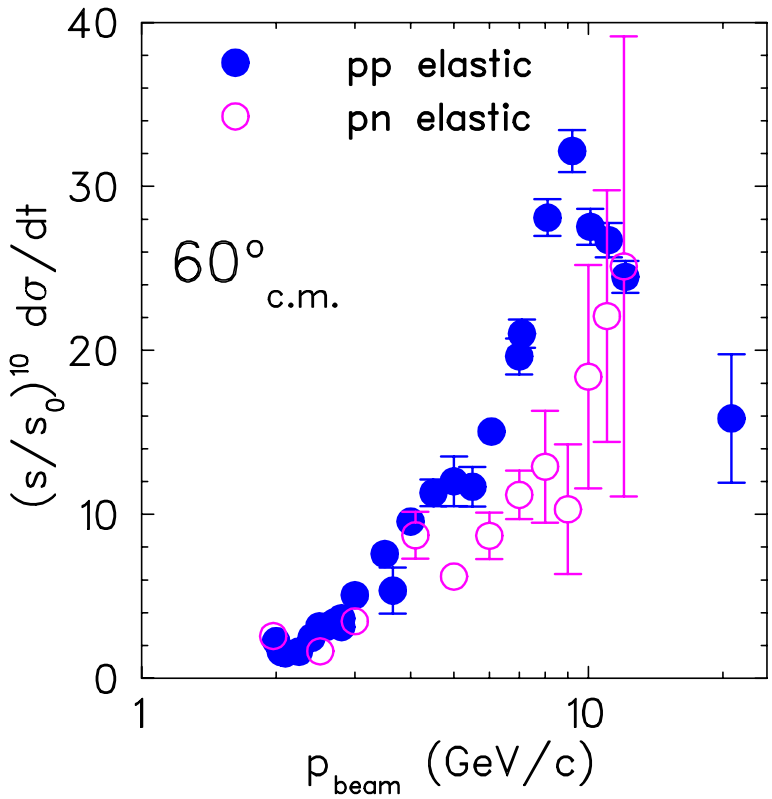

Figure 5: *Comparison of data for pp and pn elastic scattering. Data are from Ref. [26]. The cross sections have been multiplied by* $(s/s_0)^{10}$*, with* $s_0 = 13$ *GeV*^{2}*, to remove much of the energy dependence.*

1.5 Prediction for $\gamma\ ^3\mathrm{He} \to pp + n$

For high photon energy, $E_\gamma > 2 - 2.5$ GeV, the differential cross section for $\gamma\ ^3\mathrm{He} \to pp{+}n$ within the HRM can be represented as follows [27]:

$$\frac{d\sigma}{dtd^3p_n} \approx \frac{8\pi^4\alpha_{EM}}{s - M^2_{^3\mathrm{He}}}\ \frac{d\sigma^{pp}(s_{pp}, t_N)}{dt}\ \frac{1}{2}\left|\sum_{spins}\int \Psi^{^3\mathrm{He}}(p_1, p_2, p_n)\sqrt{M_N}\frac{d^2p_2}{(2\pi)^2}\right|^2, \tag{5}$$

where $s = (P_\gamma + P_{^3\mathrm{He}})^2$, $s_{pp} = (P_\gamma + P_{^3\mathrm{He}} - P_n)^2$, and $t_N \approx \frac{1}{2}(P_p - P_\gamma)^2$. The pp elastic cross section is $d\sigma^{pp}/dt$. The momentum of the recoil neutron is p_n. In the argument of the ^{3}He nuclear wave function, $\vec{p}_1 = -\vec{p}_2 - \vec{p}_n$ and $p_{1z} \approx p_{2z} \approx -\frac{p_{nz}}{2}$.

Whatever is the correct theoretical interpretation of the oscillation, if the factorization assumption holds for the hard photodisintegration of a nucleon pair, the **same oscillations should be seen** as a function of the incident photon energy. This observation is also true for the c.m. angular distribution. The unique dependence of the pp system should be transferred to the same c.m. angular dependence in the photodisintegration. **The observation of correlated oscillations in** pp **elastic scattering and** ^{3}**He pho-**

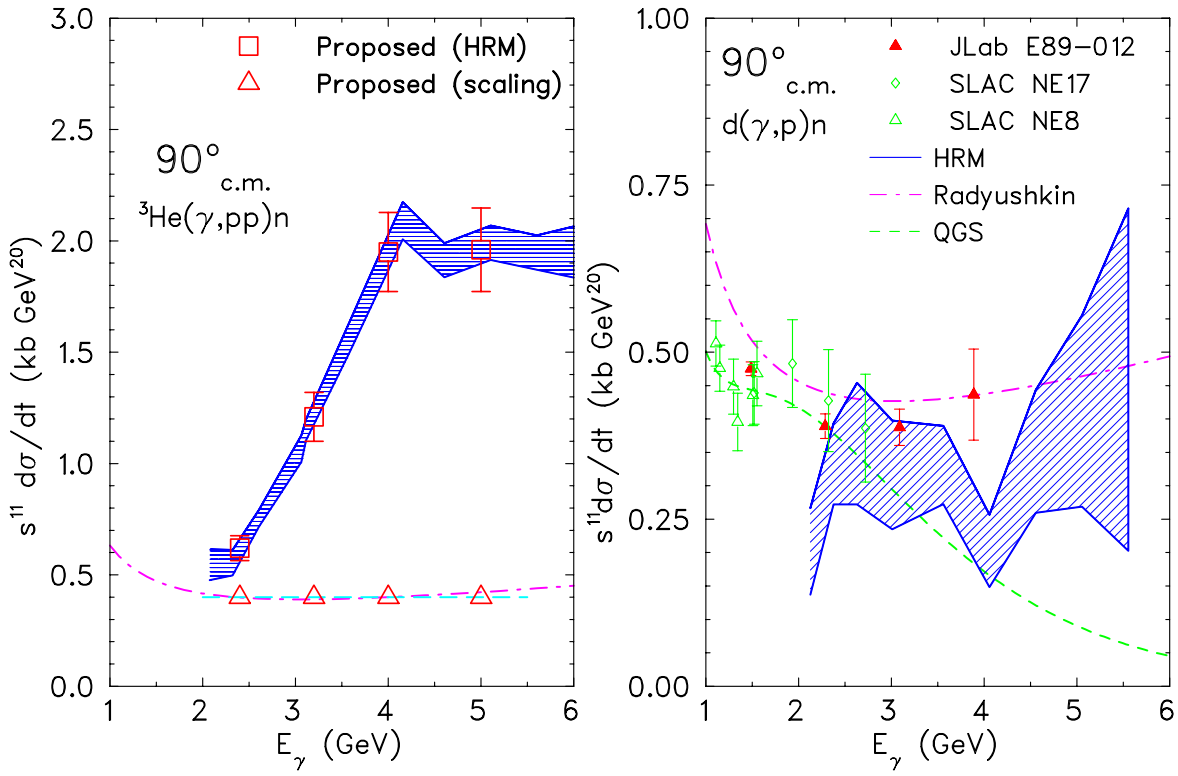

Figure 6: *The left panel shows the prediction for $\gamma\ ^3He \rightarrow pp + n$ at $\theta_{\rm c.m.} = 90°$ in the HRM as a shaded band. The dashed line is the scaling prediction, and the dot dash line shows the product of phase space times form factors. The latter two curves have been arbitrarily normalized to 0.4 at 4 GeV. The squares (triangles) show the proposed data points along with their estimated total uncertainties, assuming that the data agree with the HRM prediction with oscillations (scaling). The uncertainties are dominated by systematics – the statistical uncertainties are a factor of two to three smaller. The right panel reproduces Fig. 4 to allow a direct comparison to be made.*

todisintegration would be a clear confirmation of the factorization assumption of the HRM.

Figure 6 shows the prediction for $\gamma\ ^3\mathrm{He} \rightarrow pp + n$. Note that for Fig. 6 and Fig. 7 below, Eq. 5 has been integrated over the neutron momentum, so that the cross sections are only singly differential. The oscillation as a function of energy is very strong in the case of $\gamma pp \rightarrow pp$, leading to a much stronger predicted oscillation in ^{3}He photodisintegration than in deuteron photodisintegration. A comparison of Fig. 6 to Fig. 4 also makes it clear that the estimated uncertainty of the prediction is much smaller for the pp final state, as opposed to the pn final state. The expected precision of this proposed measurement is clearly sufficient to distinguish between the two predictions shown. The photon energy range is sufficient that we map out the full rise of the oscillation, from minimum to maximum. It should further be recalled that the onset of scaling at $\theta_{\rm c.m.} = 90°$ in

deuteron photodisintegration is at a very low photon energy, $E_\gamma \approx 1$ GeV. If these data were for deuteron photodisintegration, they would be well into the scaling regime, and suggestions of an onset of scaling at 4 GeV would not be reasonable. The transverse momentum transfer for this 4-GeV datum is nearly 2 GeV, at least 50 % greater than the p_T that characterizes the onset of scaling in $\gamma d \to pn$.

It comparing Fig. 6 to Fig. 4, it should also be noted that the absolute magnitude of the pp photodisintegration is predicted to be significantly larger than that of pn photodisintegration, in the HRM.[2] The scaling and Radyushkin curves for pp photodisintegration have been kept equal to their magnitudes for pn photodisintegration. However, Radyushkin [25] expects that the pp cross section is suppressed relative to that for pn. In Radyushkin's model, with the photon absorbed on two quarks being exchanged between the two nucleons, the cross section depends on the total charge of the exchanged quarks. For deuteron photodisintegration, the two quarks should be different flavors, e.g., a u and a d quark, leading to $p \to n$ and $n \to p$ transitions, or the interaction will be suppressed. For pp photodisintegration, the two quarks have to be the same flavor. Thus, if the pp photodisintegration cross section is similar too, or much larger than, the pn photodisintegration cross section, then Radyushkin's mechanism is not the explanation of the data.

Figure 7 shows the HRM prediction for the angular dependence of $\gamma\ ^3\mathrm{He} \to pp + n$. In contrast, data for deuteron photodisintegration tend to show a smooth variation with angle, with cross sections increasing at forward angles. The Radyushkin formula, form factors to the fourth power times phase space factors, which fits the deuteron photodisintegration angular distribution well, is also shown. To date, there is no indication of any structures in the deuteron photodisintegration angular distributions, such as shown here, but angular distributions have generally not been taken in fine enough steps with enough statistics. The proposed angular distribution points will have 3 % statistical and 5 % relative systematic uncertainties, which will be sufficient to determine if the predicted structure exists.

1.6 Nuclear corrections

The main nuclear corrections in the $\gamma^3\mathrm{He} \to pp{+}n$ reaction are due to the soft rescattering of the nucleons in the final state. The soft rescattering of the two fast nucleons on the slow spectator nucleon will introduce distortions in the picture of an isolated two proton disintegration reaction. Two type of soft rescattering can contribute to this distortion:

[2]Note that our data will also allow an extraction of the ratio of cross sections for pp and pn photodisintegration in ^{3}He. The essential point is that Monte Carlo simulations allow us to compare the measured strength in the coincidence pp spectrum to that in the singles p spectrum. Any excess strength in the singles protons arises almost entirely from pn photodisintegration. This is because the hard three-body photodisintegration cross section is likely to be very small and increasingly insignificant with energy, as it likely falls as s^{-17}.

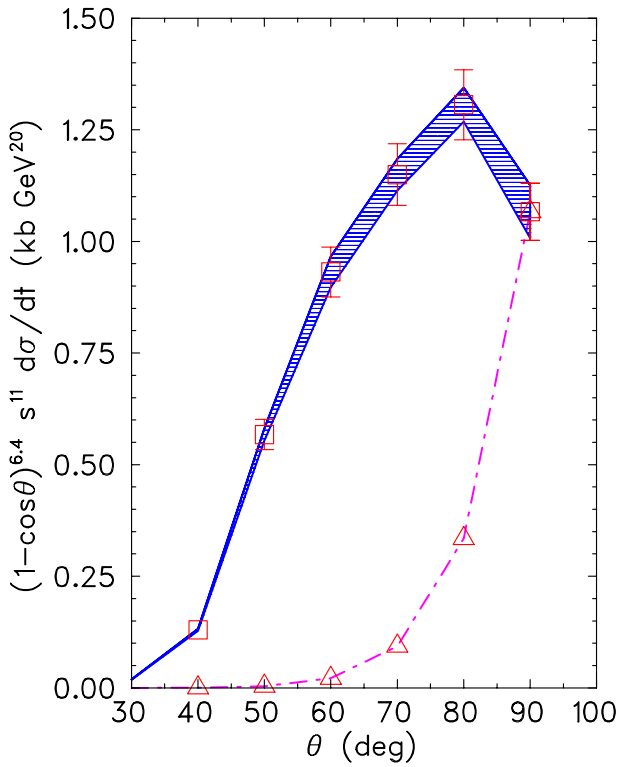

Figure 7: *The shaded band is the HRM prediction for the angular dependence of* $\gamma\,^3He \rightarrow pp + n$ *at* $E_\gamma \approx 3.1$ *GeV, compared to the proposed data points with estimated total uncertainties. The dot-dash line shows the product of phase space times form factors, normalized to give the same value as the HRM at 90°. Proposed data points with total uncertainties are shown for each of the two cases.*

- *First:* when energetic protons rescatter on the slow spectator nucleon. In this case the absorption of the protons and the distortion of the kinematics are the main source of the uncertainties. Both of these effects can be reliably calculated within the eikonal approximation since the momenta of the outgoing protons are well above the 1 GeV/c region and the momentum of the spectator nucleon is less than 100 MeV/c. The average momentum transferred during the soft rescattering is around 200 – 250 MeV/c. As a result the Glauber correction is maximal at spectator momenta $\approx$ 200 – 250 MeV/c (see e.g. [28, 29, 30, 31, 32]). Thus restricting the neutron mometa to $\leq$ 100 MeV/c significantly reduces the soft-rescattering effects. Preliminary estimations give a 5 – 10 % correction in the range of 40 – 90° c.m. angles, with the larger corrections corresponding to the smaller c.m. angles.

- *Second:* when the primary reaction happens on the *pn* pair with subsequent soft $pn \rightarrow np$ charge exchange rescattering of the energetic neutron with the slow spectator proton. This contribution again can be reliably estimated within the eikonal approximation. However it is important to note that in the energy range of this

proposal the charge exchage soft rescattering is suppressed by factor of $1/s$ as compared to the non-charge-exchange soft rescattering – here s is the c.m. energy squared of the rescattering pn system. As a result, one expects 1 – 2 % corrections due to charge exchange rescattering. Note that this estimate takes into account also the fact that one has more probability of pn than pp pairs in ^3He.

Summarizing, we emphasize that one will be able to estimate these corrections reliably since we measure in kinematics where the eikonal approximation works well for the calculation of soft rescatterings.

1.7 A measurement of the neutron spectator α distribution and a test of the scaling law in nuclei

We use here light-cone variables in which any four-momentum k can be represented as $k \equiv k(k_+, k_-, k_t)$, with $k_\pm = k_0 \pm k_z$ The z and t components are defined along and perpendicular to the direction of the incident photon beam. We also define:

$$\alpha = \frac{E - p_z}{m_A} A = \frac{k_-^N}{k_-^A} A \approx \frac{k_-}{m_N}. \tag{6}$$

With the above definitions, α for the incident photon is exactly zero for each event, independent of how accurately the photon energy is known. The conservation of α means that the α for the spectator neutron is well known for each individual event. In the $\gamma\, ^3He \to pp + n$ reaction:

$$\alpha_\gamma + \alpha_{^3\mathrm{He}} = 0 + 3 = \alpha_{p_1} + \alpha_{p_2} + \alpha_n. \tag{7}$$

Therefore:

$$\alpha_n = 3 - \alpha_{p_1} - \alpha_{p_2}. \tag{8}$$

Using the 100 MeV tip of the Bremsstrahlung beam limits the resolution of the reconstructed energy and momentum of the spectator neutron in the ^{3}He to be of the order of 100 MeV / 5 GeV = 1 %. On the other hand, the light-cone variable α can be reconstructed using Eq. 8 with a resolution which is $\sqrt{2}$ times the resolution with which the α of each detected proton is measured. With the HRS resolution, $\Delta p/p \approx 10^{-4}$ and $\Delta\,\theta \approx 1$ mr, this is at the level of 0.1 %.

The α_n value[3] also determines s for the γpp system for each event. If the factorization is verified as discussed above, the measured α distribution for the spectator neutron togther with an assumed s dependence of the $\gamma - pp$ scattering should produce the known ^{3}He wave function. This is an independent and complementary test of the in-nucleus scaling rule, Eq. 2, for the hard γNN sector.

[3]Along with p_T of the pp system, but $p_T \approx 0$ for $\theta_{\mathrm{c.m.}} \approx 90°$, and the correction is small.

1.8 Summary: goals and implications

Our goals in this proposal are threefold:

- First, we propose to map out the energy dependence of the $\gamma\ ^3\mathrm{He} \to pp + n$ process for $\theta_{\mathrm{c.m.}} = 90°$ at $E_\gamma = 2.4$, 3.2, 4, and 5 GeV, corresponding to $\mathrm{P_{beam}} \approx 6$, 7, 9 and 11 GeV/c, for comparison with the predictions shown in Fig. 6.
- Second, we propose to map out the angular dependence of the $\gamma\ ^3\mathrm{He} \to pp + n$ process at 3.2 GeV, corresponding to $\mathrm{P_{beam}} \approx 7$ GeV/c, for comparison with the predictions shown in Fig. 7.
- Third, we propose to measure the α distribution of the spectator neutron in ^{3}He, to test the scaling rule by examining moving γpp systems with different s values. This is a complementary test to the known s^{-11} dependence of the measured $\gamma - d$ hard process.

If the hard photodisintegration process can be factorized so that it depends on the NN scattering amplitude, then the oscillations apparent in pp scattering will be reflected in the measured cross sections. This result is predicted by the HRM, but not from other reaction models. It would put our understanding of deuteron photodisintegration on a firmer basis, and would be a significant step towards a general understanding of hard nuclear photoreactions at intermediate energies.

2 Experimental details

2.1 Experimental overview

We propose to measure $\gamma\ ^3\mathrm{He} \to pp + n$ in Hall A. Bremsstrahlung photons, produced by the electron beam passing through a photon radiator, will impinge on a cryogenic gas ^{3}He target. The maximum energy of the Bremsstrahlung beam is essentially equal to the incident electron kinetic energy. The target, downstream of the radiator, is irradiated by the photons and the primary electron beam. The two outgoing protons, each with about half the incident beam energy, are detected in coincidence with the two HRS spectrometers, each set for positively charged particles. We will measure the energy dependence of the differential cross section for $\theta_{\mathrm{c.m.}} \approx 90°$. We will also measure a partial angular distribution for $E_\gamma = 3.2$ GeV.

2.2 Choice of experimental hall

The need to measure a small cross section reaction that produces two high energy protons makes Hall A the only possible choice for this proposal. The experiment cannot be performed in Hall C due to the limited maximum momentum of the SOS spectrometer. The experiment cannot be performed in Hall B due to the limited luminosity available.

The basis for this statement is an extrapolation from the preliminary results of the Hall B $\gamma d \to pn$ deuteron photodisintegration experiment [6], which reached 2.5 GeV with 10° bins in the c.m. frame, and 100 MeV bins in photon energy. These data have statistical uncertainties which are about 20% at 2 GeV, and which increase with energy. Our statistical requirements, discussed below, would require nearly 2 orders of magnitude increased luminosity for a γ ^{3}He measurement in Hall B, over the γd measurement of Hall B E93-017. Thus, the statistical goals that we propose here are not feasible for a measurement in Hall B.

2.3 Beam energies and conditions

For the energy dependence of the cross sections at $\theta_{\text{c.m.}} = 90°$, a minimum beam energy of 2.4 GeV was chosen, to correspond to the estimated lower energy limit for the validity of the HRM. The angular distribution will be measured at 3.2 GeV, which corresponds to $P_{\text{beam}} \approx 7$ GeV/c. This is the lowest energy at which p_T is sufficiently large to allow reliable predictions in the HRM for a range of angles away from $\theta_{\text{c.m.}} = 90°$. There are also data for pp elastic scattering at this momentum. Thus, we propose to use beam energies of 2.4 and 3.2 GeV, with 3 and 4 pass beam at a linac energy of 0.8 GeV.

The maximum beam energy is limited by the maximum momentum of the beam right HRS spectrometer, which is ≈3.3 GeV/c, with a central momentum of 3.1 GeV/c. This limits the maximum beam energy to be about 5 GeV. We propose higher energy cross section measurements at 4 and 5 GeV, with 4 and 5 pass beam at a linac energy of about 1 GeV/pass.[4] This reduces both accelerator overhead and time needed to change the Hall A beam energy, while allowing the broadest possible energy coverage.

All requested linac energies chosen are standard. The experiment is largely compatible with concurrent G0 running in Hall C, since most of our requested beam time is at 4 and 5 GeV.

2.4 Photon radiator

The radiator is Cu with a 6% radiation length thickness.[5] To limit divergence of the beam and interactions with the target walls and flow diverters, it is preferred to use a radiator foil mounted directly in the cryotarget cell block, about 15 cm upstream of the center of the target. This compares with 73 cm upstream for the standard external Hall A radiator, and over 1 m for the Hall C radiator. During E00-007 in October 2002, it was

[4] For this photoexperiment, the exact choice of the beam energy is not critical. However, depending on the exact energy of the highest energy, 5 GeV setting, it may be necessary for this point to measure either slightly off the Bremsstrahlung end point or slightly off of $\theta_{\text{c.m.}} = 90°$ to keep the momentum of protons in the right arm consistent with the spectrometer momentum limitations.

[5] Although tagged photon beam experiments are generally desirable, the technique is not feasible for high energy, high momentum transfer reactions. The decrease in luminosity makes small cross sections unmeasureable. Our previous untagged measurements in Halls A and C have agreed well with tagged measurements, at the lower energies where an overlap is possible.

seen that it was possible to take data with this configuration even when a spectrometer, set for positive polarity, was at 20° lab, and the radiator was just entering the acceptance. The minimum angle for this proposal is ≈24° lab, and most of the measurements are taken at 40 – 50° lab. Since the radiator is directly cooled by the cryotarget, melting is not an issue. The main constraint on maximum beam current is the site boundary radiation level. We propose to do the measurement with a 50 μA beam and with the standard cryotarget raster, as has been done in earlier Hall A photoexperiments. The power deposited in the Cu is about 125 W for a beam current of 50 μA.

2.5 Target

Previous Hall A unpolarized ^{3}He experiments have used a 10 cm diameter "tuna can" cryogenic gas target, operating at $T \approx 5.8$ K, $P \approx 15$ atm, and areal density $x\rho \approx 0.81$ g/cm^2. A 20 cm long "race track" cryotarget cell is presently under construction for the HAPPEX-Helium experiment. This experiment could in principle be run with either cell. The longer, narrower cell will increase luminosity and count rates, while decreasing multiple scattering of ejected particles, leading to improved momentum and energy resolution. It is expected that it will be able to operate at the same temperature, pressure, and density as the previous cell, leading to an areal density $x\rho \approx 1.6$ g/cm^2. As the target has not yet been tested, we will assume a slightly more conservative figure of 1.4 g/cm^2 in our count rate calculations.

Note that in the kinematics of this proposal, the spectrometers only see at most the central ≈15 cm of the target. The longer target is used to reduce the uncertainty associated with cuts on and subtractions of end cap background, at the expense of slightly greater systematic uncertainty on knowledge of the acceptance vs. target position.

2.6 Spectrometers

We will use the two Hall spectrometers (HRS$_L$ and HRS$_R$) to measure two protons in coincidence. This measurement requires no changes from the standard electronics and operation of the spectrometers. For this experiment, the spectrometer momentum range is $\approx 1.3 - 3.3$ GeV/c and the angular range is 24 – 80° lab. The maximum central momentum of HRS$_R$ limits the maximum achieved s in this measurement; HRS$_L$ can be used for momenta above 4 GeV/c. All necessary equipment, including detectors, electronics, and data acquisition are available for this "standard" setup.

The desired detector stacks consist of VDCs for tracking, scintillators for triggering, and Aerogel Cerenkov detectors for rejection of small π^+ backgrounds. It is desirable, but not critical, to run without the gas Cerenkov detectors installed.

2.7 Singles trigger rates and backgrounds

Based on previous deuteron photodisintegration experiments in Hall A, the singles trigger rate is largely background triggers. The most prominant source of background at high energies is a 10 Hz rate of cosmic triggers. These cosmic events are easily removed from the data since they either miss the VDCs and give no tracks, or they hit the VDCs and, using scintillator timing information, are reconstructed to have $\beta \approx$ -1 $\pm$ 0.05. At low energies, the largest background is low energy neutral particles that give small scintillator signals, but no tracks in the VDCs. Since there are no charged particle tracks, these events are automatically removed during the analysis. They are only a problem in that the rate of these neutral events will lead to of order one hundred Hz of singles triggers in each spectrometer for the lowest energy, 2.4 GeV. We will prescale away the singles triggers by a small factor, if necessary to keep deadtime small. The relative rate of the neutral events to real photodisintegration events is very roughly independent of energy and angle. These events have not been a significant problem in singles measurements, and are less of a problem for coincidences – see below.

The rate of good charged particle tracks coming from the target is about an order of magnitude greater than the rate of protons of interest. These events come from interactions with the aluminum target cell, photodisintegration protons corresponding to lower photon energies, below the range of interest, and charged pions.

As noted above, for the angles used in this experiment, with the 20 cm long target cell, the target entrance and exit windows will not be seen by the spectrometer. If a shorter cell were used, as in previous experiments, target reconstructions would be used to remove backgrounds from the end caps. Also, the vertical flow ^{3}He target cells lack the flow diverters that run along the length of the "beer can" and machined hydrogen and deuterium target cells, removing this possible source of background. In previous deuteron photodisintegration experiments, beam interactions with the target cell have typically been 10 – 15 % of the total trigger rate. With the He cell and kinematics of this experiment, we expect this background to be negligible.

The momentum acceptance of the Hall A spectrometers typically corresponds to a 200 MeV or larger acceptance in photon energy. An event corresponding to a lower energy photon is not of interest, because the event could actually arise from a photon with a higher-than-reconstructed energy, producing an unobserved pion in the final state. These events are removed simply by reconstructing the photon energy from the two measured proton momenta, and requiring it to be close to the Bremstrahlung endpoint. In singles measurements, the reconstruction is a straightforward application of two-body kinematics. The kinematic reconstruction techniques for the coincidence measurements of this proposal are similar.

Charged π^+ mesons produced off the proton are within the acceptance. The charged pion rate observed in previous deuteron photodisintegration experiments has been about a 20% background, based on Aerogel Cerenkov cuts. In this experment, the Aerogel cut will remove most of the π^+ events, with coincidence requirements removing the rest.

2.8 Coincidence trigger rates and backgrounds

The real coincidence rate for photodisintegration events of interest is between 1 Hz at 2 GeV beam energy and 10^{-4} Hz at 5 GeV beam energy. There are few reactions that produce two positively charged high-energy particles in coincidence, and thus the measurements are generally clean.

The most important real coincidence background reactions include:

- $\gamma\, {}^3\mathrm{He} \rightarrow p\pi^+ + nn$
  The π^+ are largely suppressed in singles by an Aerogel Cerenkov pulse height cut, and are further suppressed by the coincidence time, which is 3 – 11 ns different from the pp coincidence time, depending on energy.

- $\gamma\, {}^3\mathrm{He} \rightarrow pp + n\pi^0$
  Since two protons are detected in coincidence, this reaction can only be suppressed through the use of kinematic cuts. The additional π^0 in the final state lowers the energy of the two protons, reducing the reconstructed photon energy, and changing the kinematic correlations between the two protons. Simulations show that the reconstructed α_n is large, much greater than one, allowing π^0 production events to be cleanly removed based solely on this cut. Cuts can also be placed on the reconstructed photon energy, the coplanarity of the protons, the reconstructed neutron momentum, and the transverse momentum of the pp system. [6]

The random coincidence background is not a concern, since the rates are negligible. Assuming 1 kHz single rates at the lowest energy, the random coincidence rate is about 1 KHz $\times$ 1 kHz $\times$ 100 ns = 0.1 Hz, 10 times smaller than the real rate. After cosmic events and events without tracks are removed, the random coincidence rate is reduced to 10^{-3} Hz. Requiring that the track in each spectrometer originates from the same part of the target drops the rate by about an order of magnitude to 10^{-4} Hz. Finally, requiring the events to be within a 2 ns real coincidence window lowers the rate to $2 \cdot 10^{-6}$ Hz, to be compared to the 1 Hz real rate. Since the ratio of total singles events to real photodisintegration events is very roughly independent of energy, while the random coincidence rate scales as the singles rate squared, the random coincidences become even less of a problem at higher energies.

A final background is electroproduction events. An incident electron can scatter at forward angles with very low energies, producing a high energy, high momentum, and nearly real (low Q^2) virtual photon. The pp pair can then be electrodisintegrated into two protons that have essentially identical kinematics to those of the photodisintegration events of interest. The relative rates for these processes have been checked by comparing radiator in and radiator out measurements in previous deuteron photodisintegration experiments. The data agrees well with simple estimates, and with the estimates of Tiator

[6] These are not all independent quantities, and Monte Carlo studies are being used to determine which cuts are most effective.

Table 2: *Major sources of systematic uncertainty in the experiment along with their estimated sizes.*

Systematic	Absolute	Relative
	[%]	[%]
Beam current	2	1
Photon flux	3	3
Target density	2	<1
Proton absorption in target, etc.	2	2
Spectrometer solid angle	4	1
Trigger efficiency	1	<1
Computer dead time	<1	<1
Reconstruction efficiency	1	1
Monte Carlo simulation	3	1
Background subtraction	3	3
TOTAL	8	5

and Wright [33]. The simple estimate has three parts. First, electrodisintegration acts like a 2 % radiator. Second, the target is a 2 % real photon radiator, but since it irradiates itself, its photodisintegration rate is like a $\frac{1}{2} \times 2\ \% = 1\ \%$ real photon radiator. Third, there is a 6 % real photon radiator before the target. Thus, the ratio of radiator-in to radiator-out rates is about (2 + 1 + 6) / (2 + 1) = 3. We expect to perform a limited number of measurements to verify the rate of electroproduction events.

Given the low rates expected for the experiment, we will generally be able to read out all singles and coincidence triggers, with very low data acquisition system deadtimes.

2.9 Systematic uncertainties

Our estimates of the systematic uncertainties for the cross sections are based on recent photoexperiments in Hall A. A π photoproduction experiment [34] achieved an 8 % total systematic uncertainty, and 4 % point-to-point uncertainties. As compared to this proposal, the experiment had larger cross sections, reducing the relative amount of background and thus the uncertainty in its subtraction, but had added uncertainty from estimating the π survival fraction. Deuteron photodisintegration measurements [5] had a much larger relative background, and absolute uncertainties ranged from 6 – 12 %, depending on the relative amount of background for each kinematic setting.

An estimate of the systematic uncertainties for this experiment, consistent with the recent experiments mentioned, is given in Table 2. The largest uncertainty is the solid angle for the extended target, which is nearly 4 %, as compared to closer to 1 % for a point target. The Bremsstrahlung flux adds about 3 % uncertainty to the beam flux,

Table 3: *Kinematics and estimated cross sections for the $\theta_{\rm c.m.} = 90^\circ$ excitation function.*

measurement	$E_e \approx E_\gamma$	$\theta_{\rm c.m.}$	θ_p	P_p	$\frac{d\sigma}{d\Omega}$
	[GeV]	[deg]	[deg]	[GeV/c]	[pb/Sr]
1	2.4	90	51.34	1.921	850
2	3.2	90	47.27	2.36	250
3	4.	90	44.08	2.78	65
4	5.	90	40.90	3.31	14

but this is not relevant for relative cross sections in an angular distribution. The magnitude of the background subtraction will be less for this experiment than for the singles experiment, but we estimate it will still be about 10 % of the 30 % correction for the electrodisintegration. The remaining large contribution is due to the Monte Carlo simulation. Ultimately, one has to compare Monte Carlo simulations to the experimental data, with a theoretically motivated event generator. Variations in the input will lead to slightly different distributions, fractions of events passing cuts, and cross sections. The size of the uncertainty here is assumed to be similar to that found in [34], but ultimately it will be determined by comparison of calculations to the data.

3 Requested kinematics and beam time

We propose to measure the $\theta_{\rm c.m.} = 90^\circ$ cross section at $E_\gamma = 2.4$, 3.2, 4, and 5 GeV, and an angular distribution for $E_\gamma = 3.2$ GeV at $\theta_{\rm c.m.} = 50$, 60, 70, 80, 85, and 90°. The kinematics and the predicted differential cross sections, from the HRM calculations [27], for the energy dependence and the angular distribution measurements are shown in Tables 3 and 4, respectively.

The expected count rates are presented in Table 5. Count rates have been calculated based on the following assumptions:

- The photon flux was calculated for a 6 % copper radiator using a thin radiator code. The typical number of photons is of order 10^{11} photons per second per 100 MeV photon beam energy bin per 30 μA. We used 50 μA in the time estimates.
- The target areal density is 1.4 g/cm^2, and the areal density is corrected for the length of the target seen by the spectrometer at each kinematic setting.
- The effective solid angle of each HRS spectrometer is 4 msr for the extended target.
- The efficiency for accepting two protons in the spectrometers with a neutron momentum less than 100 MeV/c reduces the effective cross section to about 50% of

Table 4: *Kinematics and estimated cross sections for the E_γ = 3.2 GeV angular distribution.*

measurement	$E_e \approx E_\gamma$	$\theta_{\text{c.m.}}$	θ_{p_1}	P_{p_1}	θ_{p_2}	P_{p_2}	$\frac{d\sigma}{d\Omega}$
	[GeV]	[deg]	[deg]	[GeV/c]	[deg]	[GeV/c]	[pb/Sr]
5	3.2	85	43.88	2.49	50.84	2.23	≈250
6	3.2	80	40.64	2.62	54.53	2.03	≈250
7	3.2	70	34.56	2.87	62.73	1.83	≈250
8	3.2	60	28.91	3.10	72.11	1.58	≈250
9	3.2	50	23.62	3.31	82.88	1.34	≈250

Table 5: *Estimated count rates.*

measurement	Energy	cross section	rate
	[GeV]	[pb/Sr]	[cnts/Hr]
1	2.4	850	500
2,5-9	3.2	250	120
3	4	65	25
4	5	14	5

the value shown in the Tables. This number is based on Monte Carlo studies using HRM calculations as input, and varies by only a few percent across our energy range.

In addition to the data runs, we propose to run about 20 % additional time without a radiator to check the background rates at all the measured conditions. The overall statistical errors will be $\leq$ 5 %, if the HRM calculations correctly predict the magnitude of the cross section. The beam time request is summarized in Table 6.

4 Related experiments

The underlying physics of this proposal for ^{3}He photodisintegration is most similar and related to several deuteron photodisintegration cross section measurements, such as Hall C E89-012 and E96-003, Hall B E93-017, and Hall A E99-008, as well as to the deuteron photodisintegration polarization measurements, Hall A E89-019, E00-007, and E00-107. These deuteron photodisintegration experiments are largely completed and there is no issue of a conflict between them and this ^{3}He photodisintegration proposal.

Table 6: *Summary of the requested beam time.*

Measurement	Time
	[hr]
Setup and efficiency calibrations	*50*
Measurement at 2.4 GeV (1000 events)	*3*
Six measurements at 3.2 GeV (1000 events)	*48*
Measurement at 4 GeV (1000 events)	*40*
Measurement at 5 GeV (500 events)	*100*
One Linac energy change and two pass changes	*16*
Four beam energy measurements	*16*
Five spectrometer angle changes at 3.2 GeV	*5*
Radiator-out measurements (20% of the radiator-in time)	*40*
TOTAL REQUESTED BEAM HOURS	*320*

There are several Hall B experiments that investigate multiparticle photo or electro-disintegration of ^{3}He or other nuclei. As discussed in the experimental details section, extrapolation from the results of the Hall B deuteron photodisintegration experiment indicates that these experiments will not be able to provide significant statistics in the kinematic region of interest to this proposal. These experiments are focused instead towards lower energies and other physics issues. An example is E93-044, "Photoreactions on ^{3}He", B.L. Berman *et al.*, which proposed to study resonances in nuclei, the three-body nuclear force, and small components of the ^{3}He wave function by using real photons of energy up to 1.5 GeV. Our lowest energy is 2.4 GeV, and we do not expect E93-044 to obtain significant statistics in the kinematics that we have proposed.

This is the only (first) proposal to measure NN outgoing particles in coincidence in hard photodisintegration of a nucleus heavier than the deuteron. Thus, we believe that there is no issue of conflicts with any other existing experiments.

5 Collaboration and needed resources

The current collaboration is composed of many members who have already performed similar photodisintegration measurements in Halls A and C, as well as members who were involved in the related Brookhaven AGS proton-proton large momentum transfer studies. This collaboration has the necessary expertise and personnel for running the experiment and analyzing the data. We are also working closely with theorists, such as Frankfurt, Miller, Sargsian, and Strikman, who motivated the proposal, assisted in its preparation, and will also help in understanding the results.

The experiment uses existing equipment at the laboratory. No new equipment is

needed. A few days of setup time in Hall A may be needed, depending on the status of the spectrometers and cryotarget prior to the start of the experiment.

References

[1] J. Napolitano *et al.*, Phys. Rev. Lett. 61, 2530 (1988); S.J. Freedman *et al.*, Phys. Rev. C 48, 1864 (1993).

[2] J.E. Belz *et al.*, Phys. Rev. Lett. 74, 646 (1995).

[3] C. Bochna *et al.*, Phys. Rev. Lett. 81, 4576 (1998).

[4] E. Schulte *et al.*, Phys. Rev. Lett. 87, 102302 (2001).

[5] E. Schulte *et al.*, Phys. Rev. C 66, 042201R (2002).

[6] P. Rossi, private communication, Hall B experiment 93-017.

[7] K. Wijesooriya *et al.*, Phys. Rev. Lett. 86, 2975 (2001).

[8] R.J. Holt, Phys. Rev. C 41, 2400 (1990).

[9] S.J. Brodsky and G.R. Farrar, Phys. Rev. Lett. 31, 1153 (1973); V.A. Matveev, R.M. Muradyan and A.N. Tavkhelidze, Lett. Nuovo Cim. 7, 719 (1973).

[10] G.P. Lepage and S.J. Brodsky, Phys. Rev. D 22, 2157 (1980).

[11] N. Isgur and C.H. Llewellyn Smith, Phys. Rev. Lett. 52, (1984) 1080; Phys. Lett. B 217, 535 (1989).

[12] A. Radyushkin, Acta Phys. Pol. B 15, 403 (1984).

[13] S.J. Brodsky and B.T. Chertok, Phys. Rev. Lett. 37, 269 (1976).

[14] G. R. Farrar, K. Huleihel and H. Y. Zhang, Phys. Rev. Lett. 74, 650 (1995).

[15] L.L. Frankfurt, G.A. Miller, M.M. Sargsian and M.I. Strikman, Phys. Rev. Lett. 84, 3045 (2000).

[16] V. Yu Grishina *et al.*, Eur. J. Phys. A 10, 355 (2000).

[17] R. Gilman and F. Gross, J. Phys. G 28, R37 (2002).

[18] D. Sivers *et. al.*, Phys. Rep. 23, 1 (1976).

[19] P.V. Landshoff and J.C. Polkinghorne, Phys. Lett. B 44, 293 (1973) and references therein.

[20] A. Hendry, Phys. Rev. D 10, 2300 (1974).

[21] B. Schrempp and F. Schrempp, Phys. Lett. 55 B, 303 (1975).

[22] J. Ralston and B. Pire, Phys. Lett. 117 B, 233 (1982).

[23] P.V. Landshoff, Phys. Rev. D10, 1024 (1974); P.V. Landshoff and D.J. Pritchard, Z. Phys. C 6, 69 (1980).

[24] S.J. Brodsky and G.F. deTeramond, Phys. Rev. Lett. 60, 1924 (1988).

[25] A. Radyushkin, private communication.

[26] M.K. Carter, P.D.B. Collins and M.R. Whalley, Compilation of Nucleon-Nucleon and Nucleon-Antinucleon Elastic scattering Data, Rutherford Appleton Lab, (RAL-86-002) 1986.

[27] M.M. Sargsian, in preparation.

[28] L.L. Frankfurt, W.R. Greenberg, G.A. Miller, M.M. Sargsyan and M.I. Strikman, Zeit. für Phys. A **352**, 97 (1995).

[29] A. Bianconi, S. Jeschonnek, N.N. Nikolaev and B.G. Zakharov, Phys. Lett. B **343**, 13 (1995).

[30] L.L. Frankfurt, M.M. Sargsian and M.I. Strikman, Phys. Rev. C **56**, 1124 (1997).

[31] S. Jeschonnek, Phys. Rev. C **63**, 034609 (2001).

[32] J.M. Laget, Nucl. Phys. A **579**, 333 (1994).

[33] L. Tiator and L.E. Wright, Nucl. Phys. A 379, 407 (1982); L.E. Wright and L. Tiator, Phys. Rev. C 26, 2349 (1982).

[34] L.Y. Zhu *et al.*, preprint nucl-ex/0211009, submitted to Phys. Rev. Lett.